TECHNICAL RESEARCH REPORT

Control of Machining Induced Edge Chipping on Glass Ceramics

by S.J. Ng, D.T. Le,
S.R. Tucker and G. Zhang

T.R. 96-3

Sponsored by
the National Science Foundation
Engineering Research Center Program,
the University of Maryland,
Harvard University,
and Industry

Control of Machining Induced Edge Chipping on Glass Ceramics

Stanley J. Ng, Dung T. Le, Shelly R. Tucker, and Guangming Zhang
Department of Mechanical Engineering & the Institute for Systems Research
University of Maryland
College Park, Maryland 20742

Abstract

Edge chipping is a phenomenon commonly observed during the machining of ceramic material. Characterization of edge chipping, both in macro and in micro scale, and correlating its formation to machining parameters form a basis for developing new and innovative technologies for controlling machining induced damage. An experimental-based study using glass ceramic material is performed. Three types of edge chipping are identified. The SEM-stereophotography method and the finite element method are used to evaluate the edge chipping effect under a set of machining conditions. Significant findings are obtained and guidelines for controlling edge chipping during machining are suggested.

1. Introduction

As new technologies merge and move forward, demands for new and advanced materials are increasing. Over the past decades, extensive research and progress have been made in the development of advanced ceramics. Advanced ceramics offer, among other outstanding characteristics, high-strength-to-mass ratio, excellent wear resistance and exceptional corrosion resistance. For these reasons, they have become prime candidates in the material selection and have penetrated almost every aspect of our daily lives.

Although the development of advanced ceramic materials has progressed tremendously over the years, barriers to their wide acceptance exist. One of these barriers is the inherent difficulty in material processing. For instance, after sintering ceramic material becomes hard and brittle. In the processing of ceramic material using traditional methods, such as machining and grinding, fracture occurs at stress-concentration locations and leaves cracks on and beneath the machined surfaces of ceramic components. These processing induced damage areas degrade the quality of products and often lead to malfunctioning and/or catastrophic failure during the period of service.

Research on processing advanced ceramics has been concentrated on the development of new and innovative machining technologies. Most of these research efforts aim at maintaining the materials' distinct features while remaining as cost-effective as possible. High speed grinding, electro-discharge machining, and laser assisted machining have been

exploited for machining ceramics with success [1-3]. Theoretical studies of deformation and fracture mechanisms of brittle solids have also made steady progress. Important criteria including the Griffith fracture criterion, the Hertzian contact fracture theory and the Irwin plastic-fracture criterion have been developed to determine the onset of the transition from a deformation process to a fracture process [4-6]. Theory of micro-scale bridging between neighboring grains during the micro-cracking along the grain boundaries has directed the development of new ceramic materials with high fracture toughness, leading to significant improvement in strength properties of ceramic components in service [7].

In this paper, we address a special type of surface and/or subsurface damage induced during the machining process, called edge chipping. Figure 1 illustrates a representative edge chipping phenomenon observed during an end milling process. Edge chipping encompasses surface damage both in macro-scale and in micro-scale. Its presence on finished products not only vitiates dimensional and geometric accuracy, but also causes possible severe failure of the ceramic component during service due to the micro-cracks left on the machined surface. Subsequently, the control of chipping effects in machining ceramic materials represents a new challenge to the manufacturing community. Research on characterizing edge chipping induced by the material processing, although not extensive, initiated as early as 1960. As reported in [8], a form tracer was used to measure the size and shape of edge chipping along the edge formed during machining. A general conclusion was made that chipping size was proportional to the material removal rate during machining. However, the previous research remained as qualitative studies, instead of quantifying the edge chipping effect.

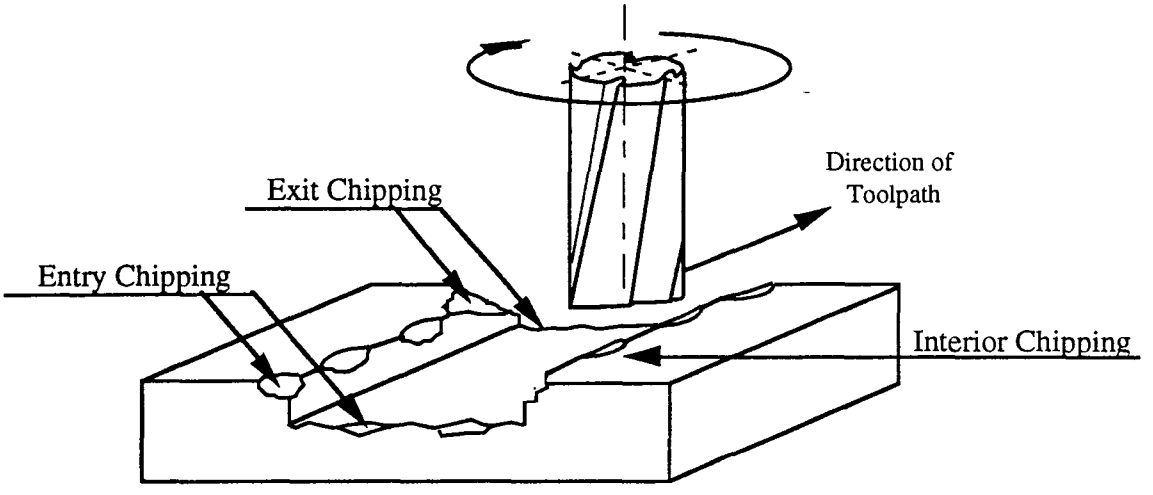

Figure1. Illustration of the Edge Chipping Phenomenon

This paper presents the characterization of three types of edge chipping in section 2, namely, the entry, interior, and exit chipping. In section 3, the SEM-stereophotography method using image processing is outlined and a non-destructive evaluation process is described to quantify the edge chipping effects under a set of selected machining conditions. The experimental investigation on edge-chipping controlled machining is given in section 4. Results from applying the finite element method to analyze the stress distribution are used to interpret the observed edge chipping phenomenon. Significant findings and guidelines for controlling edge chipping during machining are summarized in the conclusion section.

2. Characterization of Edge Chipping Phenomenon

As illustrated in Fig. 1, the formation of edge chipping initiates at the instant when the cutting tool contacts the ceramic part being machined. Edge chipping occurs on both sides along the machining path, and is present when the cutting tool leaves the ceramic part. According to the time history, the formation of edge chipping can be distinguished by three types:

(1) *Entry chipping*. Entry chipping is primarily formed during the initial impact of the dynamic loading process when the cutting tool first contacts the part material.

(2) *Interior chipping*. Interior chipping is the most dominant chipping formed in the process of material removal along the tool path.

(3) *Exit chipping*. Exit chipping is formed due to the sudden release of the stress energy, built in the part material during the machining process, at the instant when the cutting tool is leaving the part material.

As we have observed, the edge chipping remaining on the machined part can cause serious problems in fabrication due to a loss of geometric accuracy and the presence of micro cracks. It should be noted that edge chipping is a fracture mechanism. Its formation is related to the microstructures present in the part material, the size and shape of grains, and the internal stress distribution. Although edge chipping in macro-scale can be observed by careful visual examinations, edge chipping in micro-scale requires special efforts to identify its size and geometric shape characteristics.

To carry out the edge chipping study, a special type of glass ceramic material is selected. The material is called DICOR, a tetrasilicic mica glass ceramic, with a chemical formula of K_2O-MgF_2-MgO-SiO_2. The average grain size of the selected DICOR is approximately 2 μm. The material has been used for dental restorations because its physical properties closely match those of human enamel in terms of translucency, thermal conductivity, density, and hardness [9]. Some of the material properties of DICOR ceramic material are provided in Table 1.

Table 1. Properties of Dicor Ceramic

Grain Size (μm)	Density (g / cm^3)	Modulus of Elasticity (MPa)	Thermal Conductivity (W / m °C)
2	2.8	6.8×10^4	1.6

The preparation of specimens with machined surfaces is illustrated in Fig. 2. An end mill with a diameter of 3.175 mm is used to cut two blocks with dimensions of 12.7 x 12.7 x 44.5 mm^3. On each of the two blocks, four slots are machined under four different machining conditions. The four different machining conditions for slots 1-4 are combi-

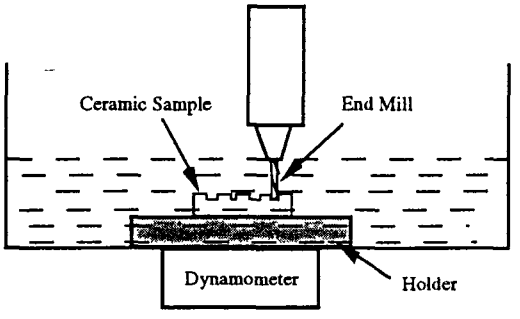

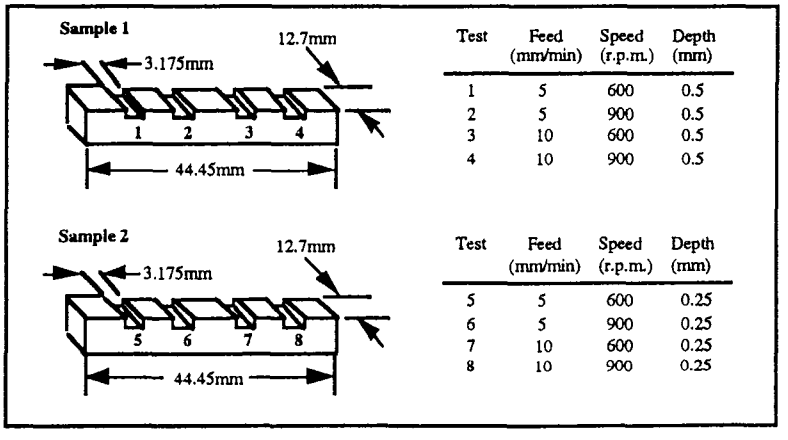

Test	Feed (mm/min)	Speed (r.p.m.)	Depth (mm)
1	5	600	0.5
2	5	900	0.5
3	10	600	0.5
4	10	900	0.5

Test	Feed (mm/min)	Speed (r.p.m.)	Depth (mm)
5	5	600	0.25
6	5	900	0.25
7	10	600	0.25
8	10	900	0.25

Figure 2. Preparation of Specimens with Machined Surfaces

nations of two feedrate settings (5 and 10 mm/min) and two spindle speed settings (600 and 900 rpm) with a constant depth of cut set at 0.5 mm [10]. When preparing slot 5-8, the feedrate and spindle speed settings remain unchanged, while the depth of cut is reduced to 0.25 mm in order to study possible effects on edge chipping due to variations in the depth of cut setting.

3. Evaluation Using SEM-Stereophotography Method

In the research of processing ceramics, great efforts have been devoted to evaluating surface integrity of the machined parts. A computer-based system has been developed for examining the micro-scale surface texture formed during the machining of ceramics. Figure 3 illustrates the basic elements of the evaluation system. The system utilizes an integration of scanning electron fractographs, image processing, stereophotography, and computer graphics [11].

As illustrated in Figure 3, a ceramic specimen with a machined surface is first examined under an environmental scanning electron microscopy (ESEM). SEM micrographs of representative damage locations on the machined surface are displayed on the screen, inspected, and digitized. Corresponding image files are then stored on computer. An image processing software tool is used to accurately obtain the length and width of the edge chipping from the image files, so as to characterize the size and shape of the edge chipping formed during machining. Numerical data in the image files denote the recorded intensity of electron reflection on the surface texture. To obtain the height information of the surface images, a gray scale-height calibration process is performed using the stereo-pair method [12]. After the SEM image data files are transformed to the height variation data files, three-dimensional topographies in micro-scale can be reconstructed using computer graphics.

Figures 4a, 4b, and 4c present the three types of chipping: the entry chipping, interior chipping, and exit chipping. Each figure provides eight representative SEM micrographs examined at the entry, interior, and exit locations, respectively. The SEM micrographs contain 640 pixels by 480 pixels, which represents a scanning area of 0.50 x 0.35 mm^2. Figures 5a and 5b present two surface topographs reconstructed in three-dimensional space using computer graphics with the transformed height variation data. The edge chipping

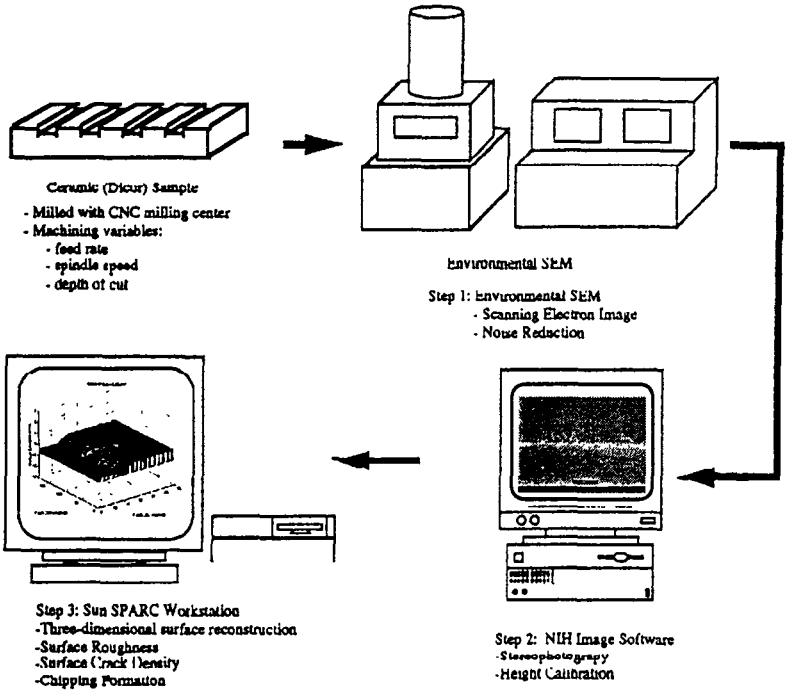

Figure 3. A Computer-Based System for Edge Chipping Characterization

topography displayed in Fig. 5a is associated with a small depth of cut, 0.25 mm, while Fig. 5b represents an edge chipping topography with the depth of cut set at 0.50 mm. A comparison of the two edge chipping topographies reveals that the edge chipping associated with the small depth of cut is significantly more severe than that associated with the large depth of cut, which clearly demonstrates the effect of depth of cut setting on the interior edge chipping formation during machining.

The size of edge chipping damage due to brittle fracture is a critical factor in assessing the machining performance for damage control. Characterization of the edge chipping sites is extremely important for correlating the edge chipping effect to the machining setting condition. In this study two quantitative measurements, i.e., the length and the width of edge chipping are used to characterize the interior edge chipping phenomenon, which constitutes a dominant portion of all edge chipping in the slot milling process. Because a noticeable difference of the interior edge chipping on the left and right sides exists, data are taken on both sides and recorded. A ratio of the measured length to the measured width, denoted as the aspect ratio, is then calculated. Table 2 lists the measured and calculated data for subsequent analyses.

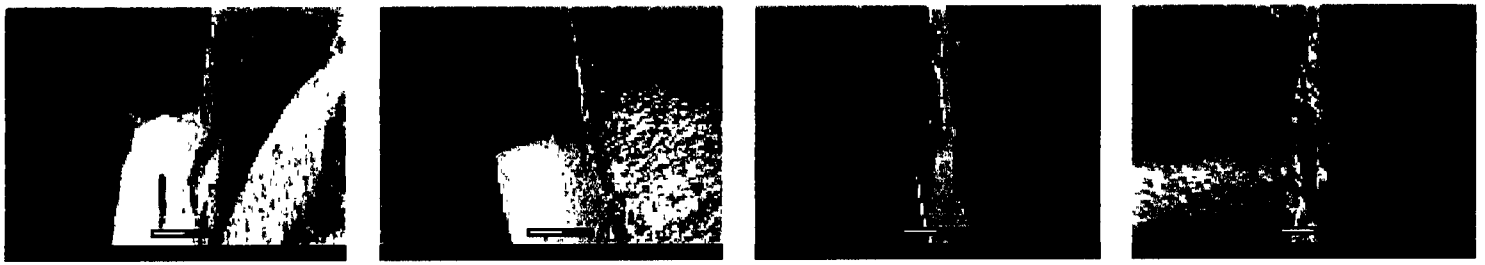

Slot 1
Cutting Speed = 600 rpm
Feed = 5 mm/min
Depth of Cut = 0.50 mm.

Slot 2
Cutting Speed = 900 rpm
Feed = 5 mm/min
Depth of Cut = 0.50 mm

Slot 3
Cutting Speed = 600 rpm
Feed = 10 mm/min
Depth of Cut = 0.50 mm

Slot 4
Cutting Speed = 900 rpm
Feed = 10 mm/min
Depth of Cut = 0.50 mm

Slot 5
Cutting Speed = 600 rpm
Feed = 5 mm/min
Depth of Cut = 0.25 mm

Slot 6
Cutting Speed = 900 rpm
Feed = 5 mm/min
Depth of Cut = 0.25 mm

Slot 7
Cutting Speed = 600 rpm
Feed = 10 mm/min
Depth of Cut = 0.25 mm

Slot 8
Cutting Speed = 900 rpm
Feed = 10 mm/min
Depth of Cut = 0.25 mm

Figure 4. a) SEM Micrographs of the Entry Edge of the Ceramic Specimen

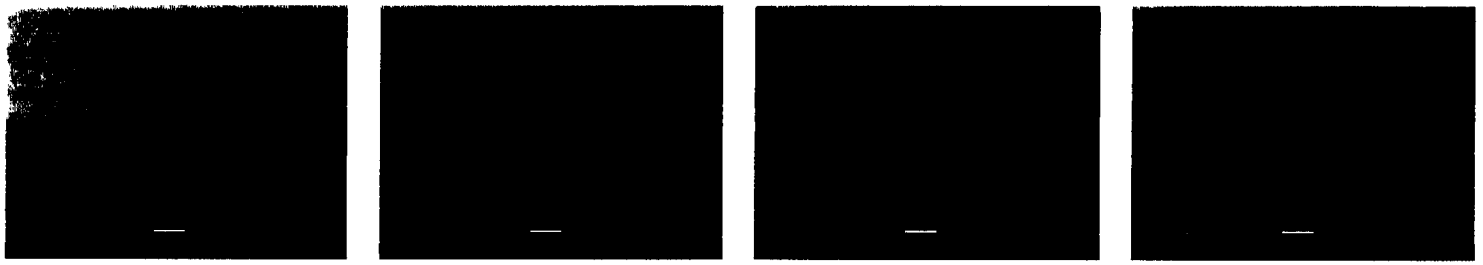

Slot 1		Slot 2		Slot 3		Slot 4	
Cutting Speed	= 600 rpm	Cutting Speed	= 900 rpm	Cutting Speed	= 600 rpm	Cutting Speed	= 900 rpm
Feed	= 5 mm/min	Feed	= 5 mm/min	Feed	= 10 mm/min	Feed	= 10 mm/min
Depth of Cut	= 0.50 mm.	Depth of Cut	= 0.50 mm	Depth of Cut	= 0.50 mm	Depth of Cut	= 0.50 mm

Slot 5		Slot 6		Slot 7		Slot 8	
Cutting Speed	= 600 rpm	Cutting Speed	= 900 rpm	Cutting Speed	= 600 rpm	Cutting Speed	= 900 rpm
Feed	= 5 mm/min	Feed	= 5 mm/min	Feed	= 10 mm/min	Feed	= 10 mm/min
Depth of Cut	= 0.25 mm	Depth of Cut	= 0.25 mm	Depth of Cut	= 0.25 mm	Depth of Cut	= 0.25 mm

Figure 4. b) SEM Micrographs Along the Machined Slot of the Ceramic Specimen

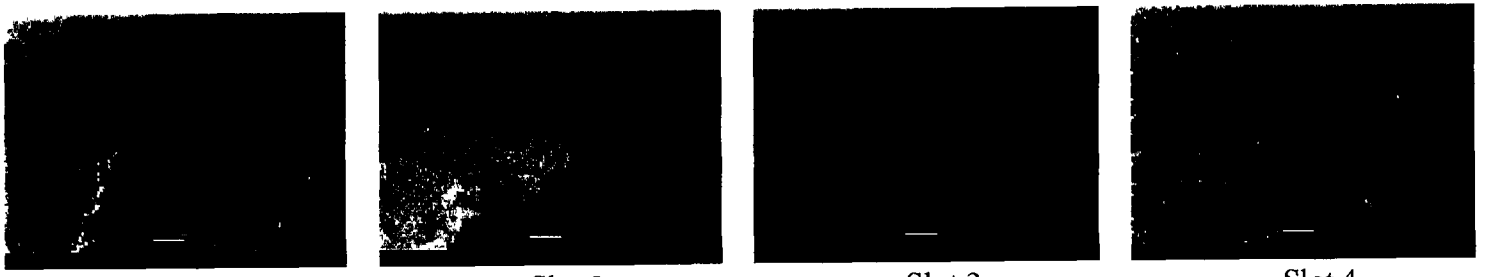

Slot 1
Cutting Speed = 600 rpm
Feed = 5 mm/min
Depth of Cut = 0.50 mm.

Slot 2
Cutting Speed = 900 rpm
Feed = 5 mm/min
Depth of Cut = 0.50 mm

Slot 3
Cutting Speed = 600 rpm
Feed = 10 mm/min
Depth of Cut = 0.50 mm

Slot 4
Cutting Speed = 900 rpm
Feed = 10 mm/min
Depth of Cut = 0.50 mm

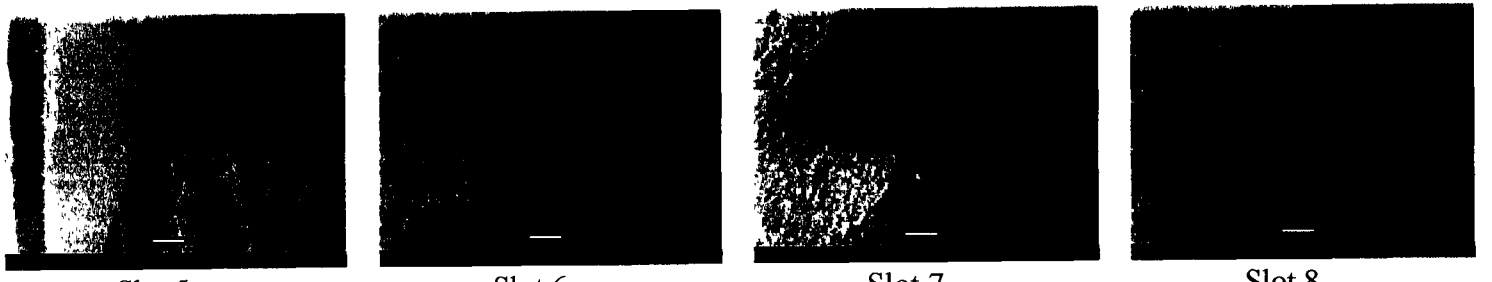

Slot 5
Cutting Speed = 600 rpm
Feed = 5 mm/min
Depth of Cut = 0.25 mm

Slot 6
Cutting Speed = 900 rpm
Feed = 5 mm/min
Depth of Cut = 0.25 mm

Slot 7
Cutting Speed = 600 rpm
Feed = 10 mm/min
Depth of Cut = 0.25 mm

Slot 8
Cutting Speed = 900 rpm
Feed = 10 mm/min
Depth of Cut = 0.25 mm

Figure 4. c) SEM Micrographs of the Exiting Edge of the Ceramic Specimen

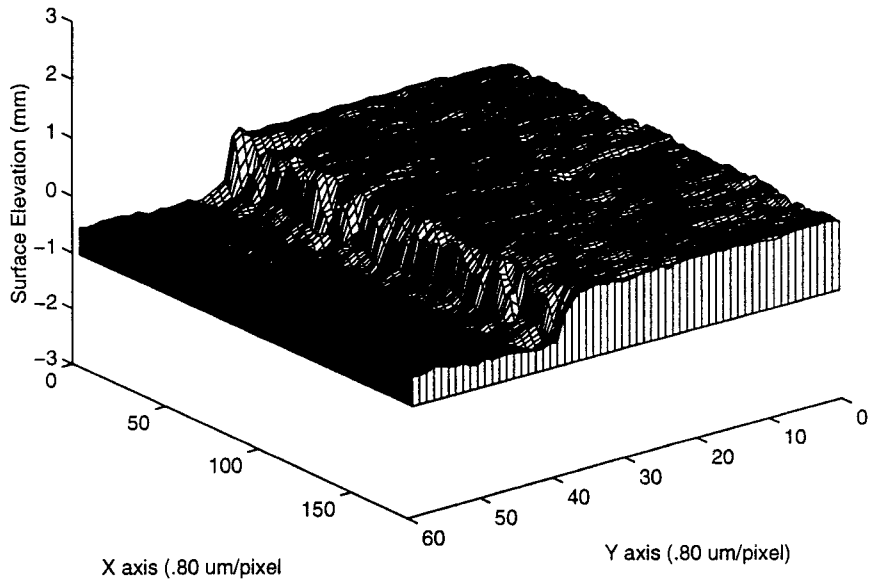

a) Slot 1 (Depth of Cut = 0.50 mm)

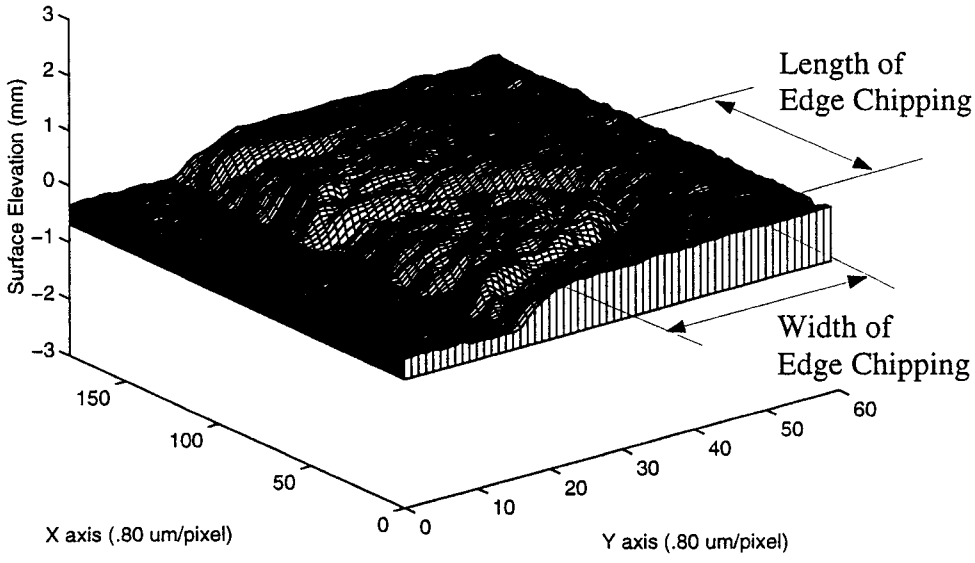

b) Slot 5 (Depth of Cut = 0.25 mm)

Figure 5. Three Dimensional Reconstructed Topography of the Machined Edges

Table 2. Results of Chip Length, Width and Aspect Ratio Evaluation

Slot Number	1	2	3	4	5	6	7	8
Chip Length (μm)	40.7 (30.2) (51.2)	40.2 (36.3) (44.1)	46.1 (35.8) (56.4)	76.1 (58.7) (93.5)	102.6 (62.0) (143)	101.0 (83.6) (118)	106.4 (60.8) (152)	169.8 (123) (216)
Chip Width (μm)	13.2	12.8	15.7	27.4	37.3	39.0	37.2	56.4
Aspect Ratio (L/W)	3.0	3.3	3.2	3.0	2.8	2.6	3.0	3.2

3.1 Evaluation of the Length of Edge Chipping

The data listed in the second row of Table 2 represents the lengths of the edge chipping for the eight machining conditions. The average of the first four numbers, associated with a depth of cut equal to 0.50 mm, is 50.8 μm, and the average of the second four numbers associated with a depth of cut equal to 0.25 mm is 120.0 μm, as calculated below. Thus, the effect of depth of cut on the edge chipping length is evident. A small depth of cut setting will induce interior edge chipping with a large length.

$$\frac{40.7 + 40.2 + 46.1 + 76.1}{4} = 50.8 \quad (\mu m)$$

$$\frac{102.6 + 101.0 + 106.4 + 169.8}{4} = 120.0 \quad (\mu m)$$

The two circled numbers listed below each edge chipping length value in the second row represent the lengths of the edge chipping on the right and left sides of the respective slot. Although each side of the slots was subjected to identical machining conditions, the numerical data on the right side is consistently larger than that on the left side, indicating an effect of the direction of end milling rotation on edge chipping. Figure 6 offers the explanation of this effect, which is derived from the configuration of cutting geometry during the material removal process. As illustrated, the thickness of cut on the right side is significantly larger than that on the left side. Consequently, the cutting force generated during machining will be significantly larger while machining the right side, as compared to the magnitude of the cutting force generated while machining the left side. It is well understood that a large external force induces a strong internal stress field in the part

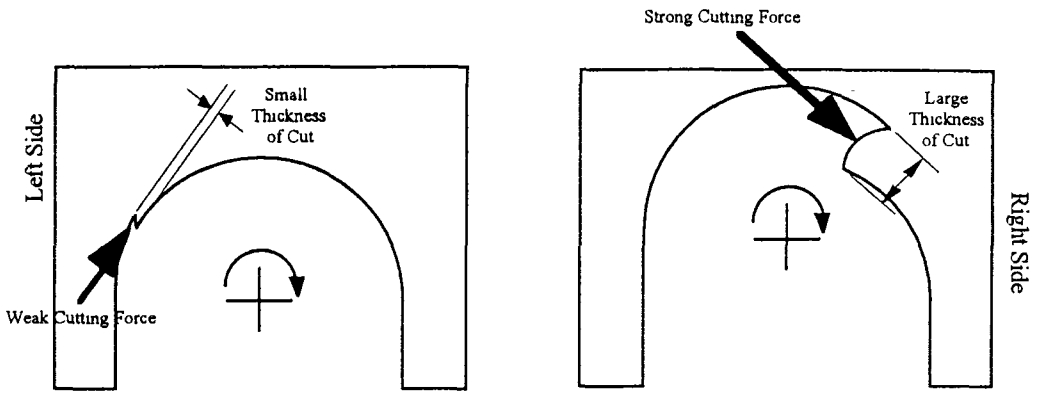

Figure 6. Effect of the Direction of End Mill Rotation on Edge Chipping

material being machined, thus leading to severe stress concentration and greater edge chipping thereafter.

In order to correlate the edge chipping effect to the machining parameter settings, an empirical model is derived from the data listed on the second row in Table 2. It is given by

Chip Length = 85.4 + 22.8 (Spindle Speed) - 69.2 (Depth of Cut) + 28.5 (feed)

The three coefficients listed in the model, +22.8, -69.2, and +28.5, characterize the effects of three parameters on the length of edge chipping. The two positive signs mean that the length of edge chipping will increase as spindle speed and feed increase. On the other hand, the negative sign with depth of cut indicates a large depth of cut setting tends to reduce the length of edge chipping. The derived empirical model is very useful for providing guidelines in setting the machining parameters during the machining of ceramic materials.

3.2 Evaluation of the Aspect Ratio of Edge Chipping

Examining the aspect ratio data listed in Table 2, an important observation is that the aspect ratio remains almost constant with small variation about the mean value of 3. This indicates that the edge chipping with large length is usually associated with large width, and the edge chipping with small length associated with small width. Consequently, the volume of individual edge chipping locations, or individual edge chipping cavities, varies

in a specific pattern as they jump from one value to another. This phenomenon indicates that the formation of edge chipping is related to certain inherent properties of the material being machined. Among them, the microstructural characteristics are more likely to be responsible. These characteristics include the grain size, weak grain interfaces, and volume fraction of the second phase.

3.3 Evaluation of the Cavity Density of Edge Chipping

In order to gain a comprehensive understanding between the fracture mechanism present during machining and the formation of edge chipping, a special effort is made. The method of contour mapping is used to evaluate the cavity density, a performance index defined to characterize the third dimension of edge chipping.

Examining the two reconstructed surface topographies shown in Figs. 7a and 7b, they represent two visualized edges formed during the machining of the two slots, i.e., slot 1 and slot 5, respectively. As depicted, the extent of chipping generated damage on slot 1 is much more severe than that on slot 5 because it has a much larger chipping size formed. Note the scale used in the visualization. In the marked X and Y axes, each pixel represents 0.8 μm, and the indicated area 160 pixels by 80 pixels represents an actual area of 128 μm x 64 μm. The unit of the vertical axis is also in micrometer.

To quantify the surface texture of the chipped edges, contour plots are taken at six levels on the vertical direction. They are 0 mm, -0.1 mm, -0.2 mm, -0.3 mm, -0.4 mm and -0.5 mm with the level 0 mm representing the reference plane for material removal, as illustrated in Figs. 7a and 7b. Figures 8a and 8b present the two assembled contour maps for the two chipped edges of slot 1 and slot 5, respectively. On the these contour maps, the grain size of 2 μm is also indicated as reference for examination. Important observations are listed as follows:

(1) The size of the chipping formed varies as the machining condition varies. In Fig. 7a, the corresponding cutting condition are cutting speed: 600 rpm, feed rate: 5 mm/min, and depth of cut: 0.5 mm. The average chipping size, as indicated by those small isolated islands formed by clustered contour lines on the contour map, is 8 μm x 2.4 μm at -0.2 mm level. In Fig. 8b, while maintaining the same cutting speed and feed rate, a smaller depth of cut, 0.25 mm, is used. The average chipping size increases to 96 μm x 40 μm, indicating severe edge chipping as discussed previously. It is interesting to note that the smallest size of edge chipping

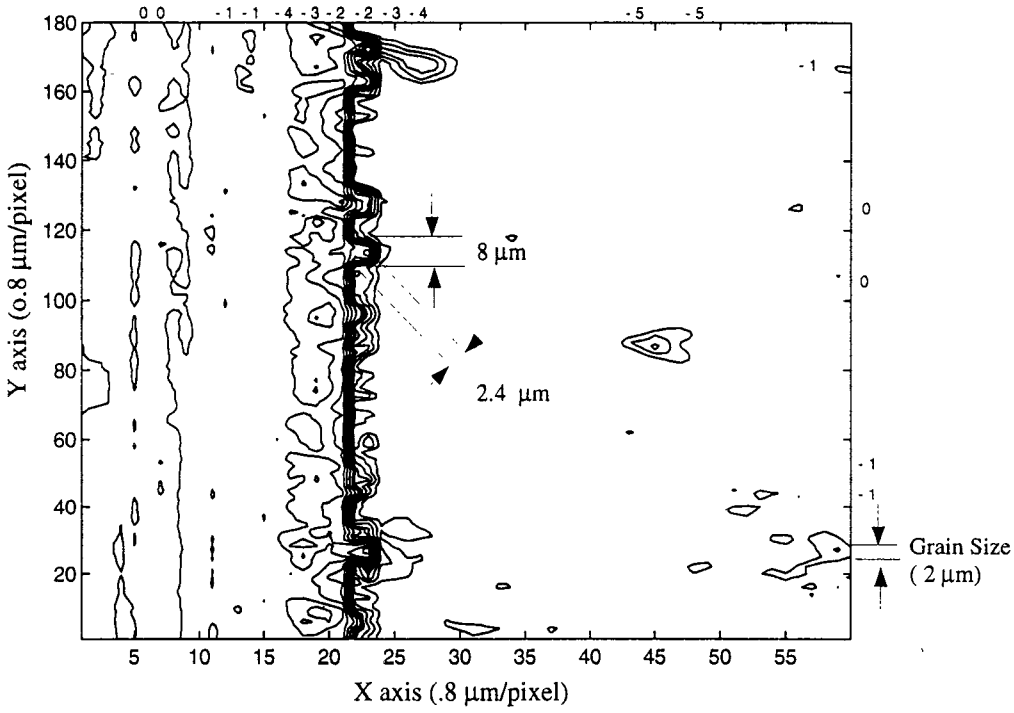

a) Slot 1(Chip Size Evaluated at -02mm)

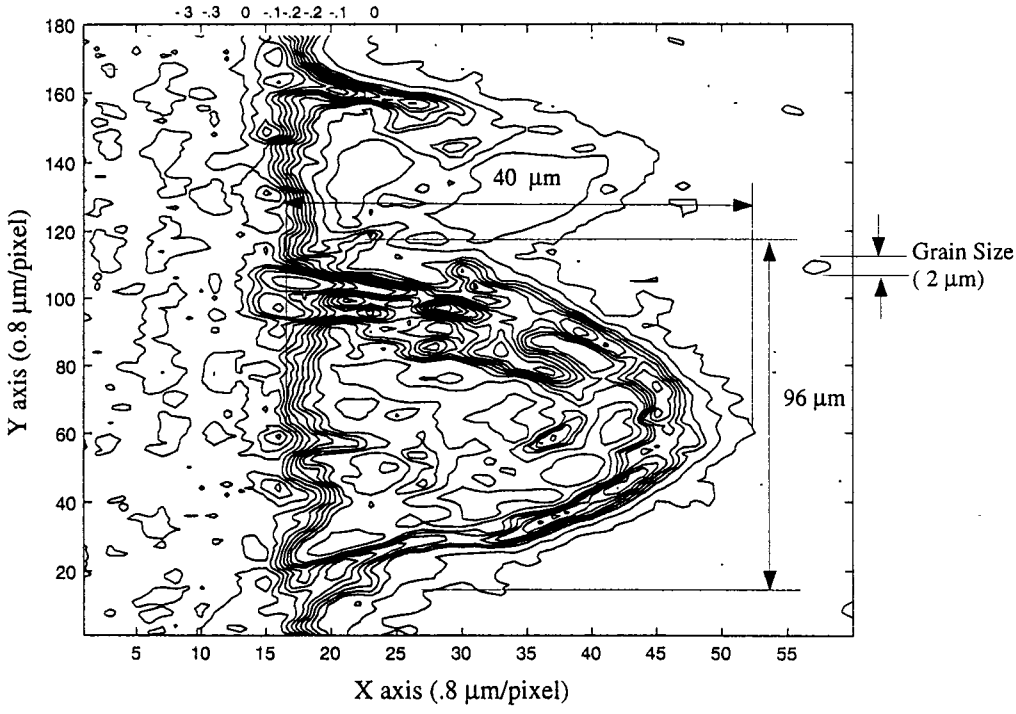

b) Slot 5 (Chip Size Evaluated at -02 mm)

Figure 7 Assembled Contour Maps of the Machined Edge Topography

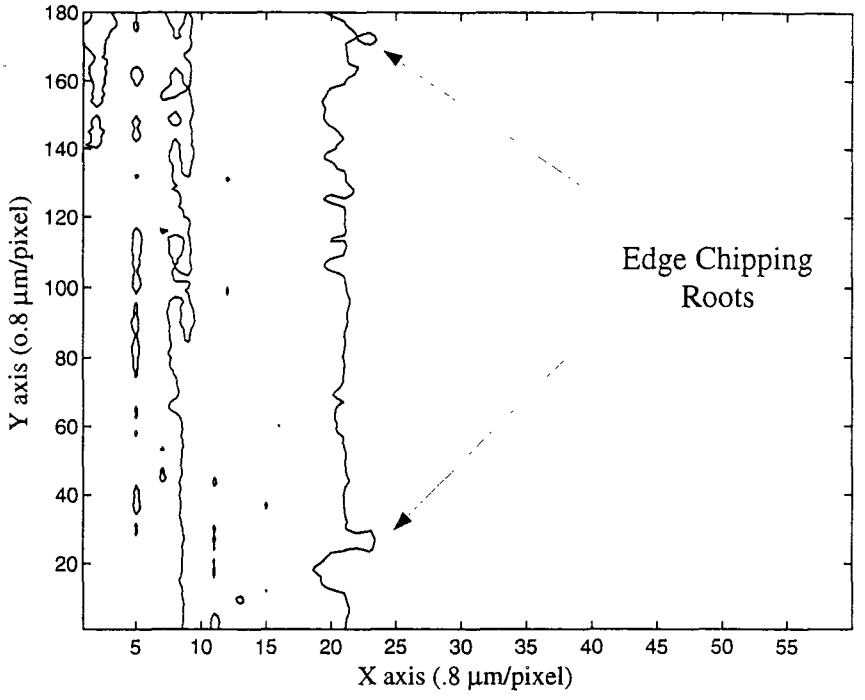

a) Slot 1(Elvation Level = -0.35 mm)

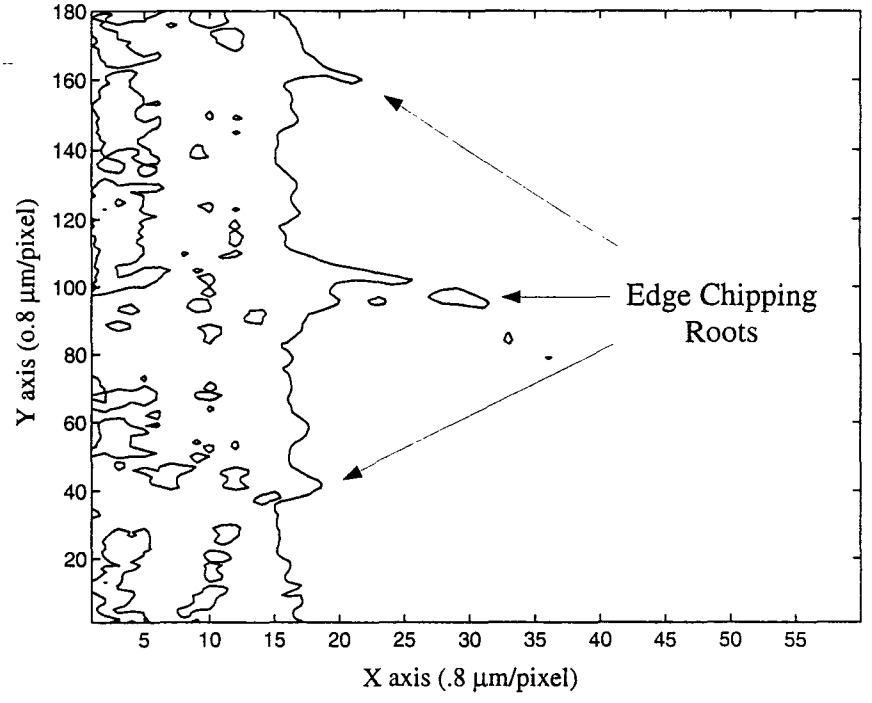

b) Slot 5 (Elevation Level = -0.25 mm)

Figure 8 Contour Maps of the Machined Edge Topography Illustating Roots of Edge Chipping

on both maps is about 2 μm, which is about the grain size of DICOR material used in this study. This observation suggests the existence of pullouts of a single grain during machining. It is well understood that grain boundaries in DICOR material represent a weak interface when subjected to a tensile stress field due to the presence of second phase - mica flakes. Edge chipping with small sizes can be due to the dislodgment of individual grains. On the other hand, macro-scale edge chipping is mainly caused by intergranular fracture along multi-grain boundaries.

(2) The density of contour lines surrounding the isolated islands characterizes the depth of edge chipping. To quantify the depth of the edge chipping, contours are constructed as the elevation level goes down toward the machined surface. Figures 9a and 9b are the two contour maps, on which the edge chipping almost disappears, indicating the location of the edge chipping root. The two relative distances between the contour map and the machined surface are marked on Figs. 8a and 8b, which are 0.35 mm and 0.25 mm, respectively. If comparing the distance with the depth of cut setting for slot 5 which is equal to 0.25 mm, it is evident that the edge chipping starts at the corner of the end milling tool where stress concentration is built up. Cracks are formed and then propagated upward. When the crack propagation reaches the free-surface of the part material, edge chipping occurs. However, for the case of a large depth of cut setting, the crack propagation has its limit. The built-up strain energy may not be sufficient enough to allow the crack propagation reaching the free-surface.

4. Control of Edge Chipping during Machining

Control of edge chipping on the shop floor and/or on clinic sites is a major issue during the machining of DICOR material. For the three types of edge chipping, different approaches should be applied. For instance, controlling the direction of end mill rotation may represent an effective and economic way to minimize the interior edge chipping effect as long as the side with severe edge chipping is removed after machining. In this paper we present a new approach to control the edge chipping at both entry and exit locations.

4.1 Addition of Epoxy Material at the Entry and Exit Locations

The basic methodology employed in the new approach is illustrated in Fig. 8. Epoxy material is used to construct a sandwich structure, in which the glass ceramic specimen is placed between two epoxy blocks. Such a design follows two considerations:

1. providing an energy buffer to prevent sharp impact at the entry location; and

2. providing additional support to back the ceramic material at the exit location.

Note that the two epoxy blocks shown in Fig. 8 cover the left portion of the ceramic specimen only. The right portion remains unsandwiched. This special arrangement allows a side-by-side comparison to determine whether the added epoxy material attenuates the entry edge chipping and/or the exit edge chipping during machining.

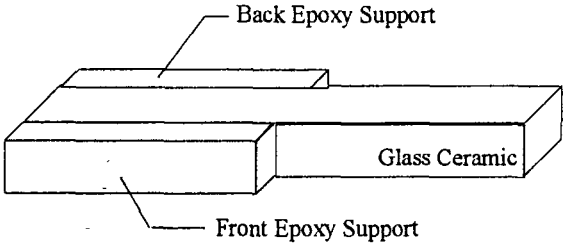

(a) Before Machining

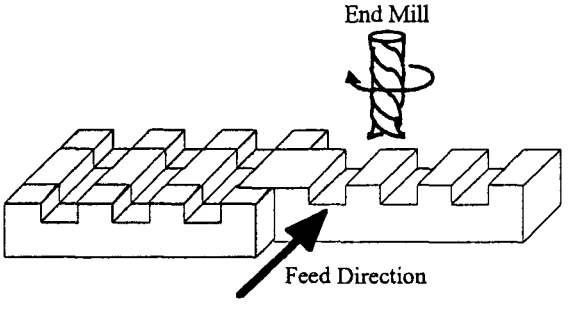

(b) After Machining

Figure 8. Addition of Epoxy Material to the Ceramic Specimen

4.2 Experimental Investigation

The experimental investigation using the specimen with the epoxy material blocks to study possible protection of edge chipping consists of two steps:

Step 1: Duplicates of slots are machined with identical cutting parameter settings. As illustrated in Fig. 8, three slots are machined on the left portion and three slots are machined on the right portion. The cutting parameter settings are: spindle speed = 900 rpm, feed rate = 0.005 m/min, and depth of cut = 0.25 mm. An end mill with a diameter of 3.175 mm is used.

Step 2: After machining, the edge chipping effects at the entry and exit locations are examined under the environmental scanning electron microscope (ESEM). Four micrographs, which are representative of the edge chipping damage, are shown in Fig. 9. The top two micrographs show the entry edge chipping and the exit edge chipping without the epoxy block support. The two micrographs below them are taken from the left portion where additional support with the epoxy blocks is present during machining.

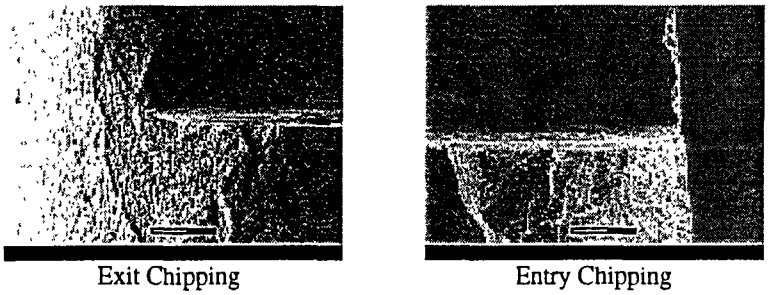

Exit Chipping Entry Chipping

(a) Without Epoxy

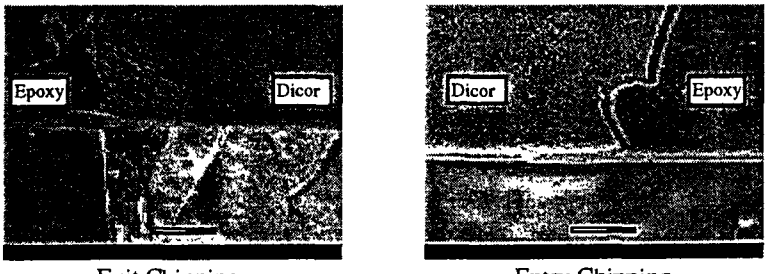

Exit Chipping Entry Chipping

(b) With Epoxy

Figure 9. Comparison of Edge Chipping at the Entry and Exit Locations with/without Presence of Epoxy Blocks

Examining the two micrographs at the entry location, significant reduction of edge chipping when epoxy block was present during machining can be observed. This concludes that, serving as a buffer, the epoxy material absorbed the impact energy and a smooth transition of the end mill from leaving the epoxy material to entering the ceramic material was achieved.

Examining the two micrographs at the exit location, the edge chipping with presence of the epoxy block is as severe as that without the epoxy block support. Figure 10 presents an enlarged view of the exit edge chipping with presence of the epoxy block. The interface between the epoxy material and the ceramic specimen is marked. A micro-scale gap on the interface can be observed. Micro cracking on the ceramic specimen is clearly depicted in the area Just before the gap. These observations indicate that there exists discontinuity on the interface in terms of the energy transition from the ceramic part to the epoxy block. Figure 11b qualitatively describes that a small portion of the built-up strain energy is transferred to the epoxy block and a significant portion of the built-up strain energy is lost on the interface. The lost energy is converted to surface energy in the process of micro-cracking at the exit location.

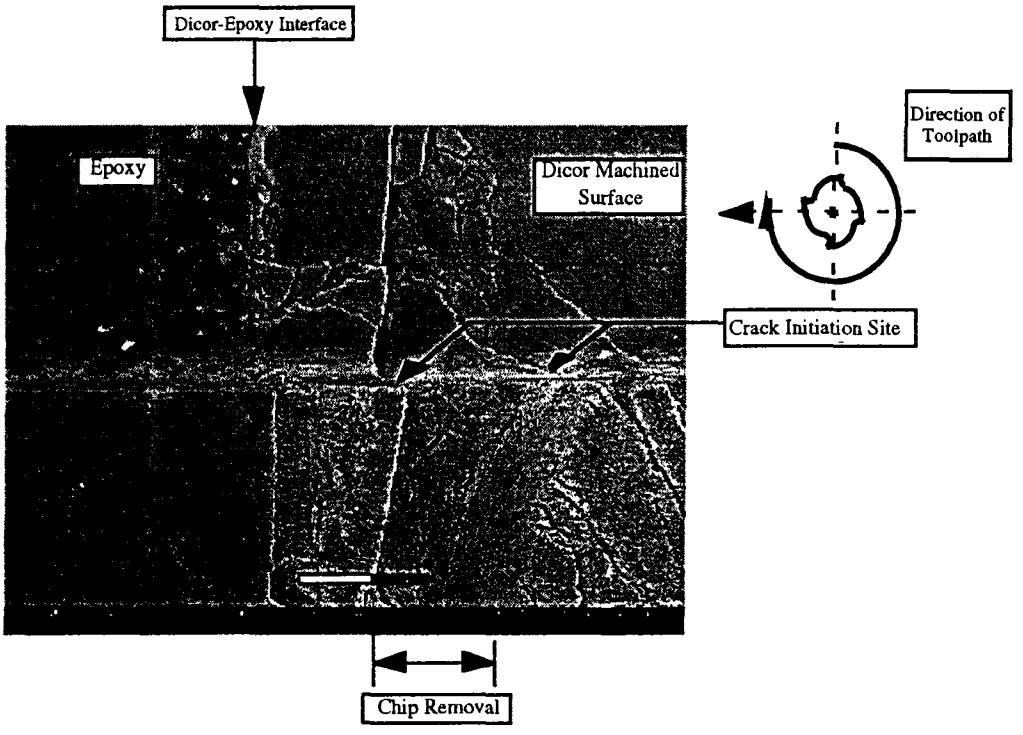

Figure 10. Micro-Cracking on Interface between the Ceramic Specimen and the Epoxy Block

4.3 Analysis Using Finite Element Method

It is interesting to note that the edge chipping on the left side of the slot is much more severe as compared with that on the right side. It might be contrary to what has been observed from the interior edge chipping effect, in which the edge chipping on the left side of the slot is much less severe than that on the right side. To gain a comprehensive understanding, an analysis using finite element method is conducted. Figure 11a presents the mesh generation and the induced stress distribution obtained from the finite element analysis. The distribution illustrates the concentration of tensile stress at the left corner at the exit location and the compressive stress at the right corner. Note that the cutting force acting at the right corner is significantly reduced at the exit location because of the reduction of thickness of cut, considering the fact that the end mill is rotating from the air to contacting the ceramic specimen when it cuts the right corner.

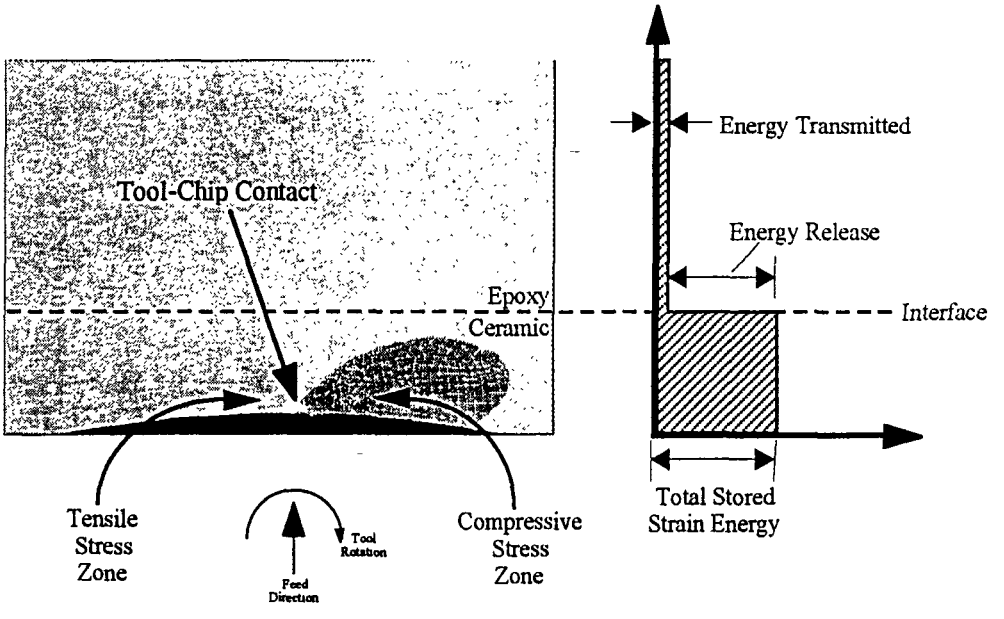

(a) Induced Stress Distribution (b) Energy Distribution

Figure 11. Analysis Using Finite Element Method and Energy Distribution on the Interface

5. Conclusions

A combined analytical and experimental study has been performed in this research with focus on edge chipping, a phenomenon commonly present during the machining of ceramic material. Glass ceramic material is used under the milling operation. Significant findings are summarized as follows.

1. Edge chipping can be categorized in three types, namely, the entry edge chipping, the interior edge chipping, and the exit edge chipping according to the time history of formation.
2. A developed SEM-Stereophotography system has been used to study the formation of edge chipping through three-dimensional visualization. In this research the interior edge chipping is characterized by its length, width and the ratio of length to width. Correlation between edge chipping and machining parameter settings has been established, indicating a noticeable effect of depth of cut on the edge chipping formation.
3. An effort has been made to search a methodology to control the edge chipping formation during machining. Epoxy material is used to provide additional support to the specimen being machined. Effectiveness of reducing the entry edge chipping has been achieved. However, no effect has been observed to control the exit edge chipping due to discontinuity of energy transformation on the interface.
4. Results from the finite element analysis strongly indicate that the microstructure, induced stress distribution, and weak boundaries due to presence of second phase are key factors, which have direct connection to the edge chipping formation during machining.

Acknowledgment

The authors acknowledge the support from the University Research Board, the Mechanical Engineering Department, and the Institute for Systems Research under NSFD CDR-88003012 grant. Part of the support is also provided through NIH grant P1DE10976A. Special thanks are due Dr. Dianne Rekow at the University of Medical and Dentistry of New Jersey, and to the Defense Acquisition Scholarship Program office of the Department of Defense for their support of this work. The authors also express gratitude to Mr. Lenox S. Job for his unique contribution.

References

[1] Konig, W., et al, "Machining of New Materials," Processing of Advanced Materials, Vol. 1, 1991, pp. 11-26.

[2] Mazurkiewicz, M., "Understanding Abrasive Waterjet Performance," Machining Technology, Vol. 2, No.1, 1991, pp. 1-3.

[3] Inasaki, I., "Grinding of Hard and Brittle Materials," Annals of the CIRP, Vol. 36 (2), 1987.

[4] Irwin, G.R., "Fracture Dynamics," Fracturing of Metals, American Society of Metals, Cleveland, OH, 1948.

[5] Irwin, G.R., et al., "Fracturing and Fracture Dynamics," Welding Journal, Vol. 31, Research Supplement, pp. 95s-100s, 1951.

[6] Griffith, A.A., " The Phenomena of Rupture and Flow in Solids," Philosophical Transactions of the Royal Society (London), 221, pp. 163-198, 1921.

[7] Lawn, B., Fracture of Brittle Solids, Second Edition, Cambridge University Press, 1994.

[8] Ohbuchi, Y., et al., " Chipping Generation Mechanism in Slot Grinding of Ferrite," Int. J. Japan Soc. Pre. Eng. , Vol.28 , No.1, Mar. 1994.

[9] Grossman, D.G., "Structure and Physical Properties of Dicor/MGC Glass-Ceramic," Proceedings of the 1991 International Symposium on Computer Restorations, Regensdort-Zurich, Switzerland, 1991, pp. 103-115.

[10] Zhang, G., et al., "Characterization of Surface Texture Formed During Machining of Ceramics", NAMRC Publication, 1995.

[11] Stout, K.J., ed., Three Dimensional Surface Topography; Measurement, Interpretation, and Applications, Penton Press: London, England, 1994.

[12] Goldstein, J., et al., Scanning Electron Microscopy and X- Ray Microanalysis, Plenum Press: New York, Second Edition, 1992.

[13] ANSYS General Purpose Finite Element Analysis (FEA) program, Revision 5.0, Swanson Analysis Systems, Inc., 1992.